1995

Lower Palaeozoic sedimentology and stratigraphy of the Kerman region, East-Central Iran

Mir Alireza Hamedi
University of Wollongong

LOWER PALAEOZOIC SEDIMENTOLOGY AND STRATIGRAPHY OF THE KERMAN REGION, EAST-CENTRAL IRAN

A thesis submitted in fulfilment of

requirements for the degree of

DOCTOR OF PHILOSOPHY

from

THE UNIVERSITY OF WOLLONGONG

NEW SOUTH WALES

AUSTRALIA

by

MIR ALIREZA HAMEDI

(BSc *Mashhad*, MSc *Wales, U.K.*)

DEPARTMENT OF GEOLOGY

1995

DEDICATION

I dedicate this thesis to my parents, my wife Ghodsi, my son Hussein and my daughter Maryam.

Except where otherwise acknowledged, this thesis represents the author's original research, which has not previously been submitted to any institution in partial or complete fulfilment of another degree.

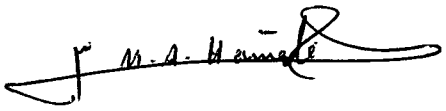

M. A. HAMEDI

June 1995

THE UNIVERSITY OF WOLLONGONG

DECLARATION RELATING TO DISPOSITION OF THESIS - PhD

This is to certify that I, **MIR ALIREZA HAMEDI**, being a candidate for the degree of **DOCTOR OF PHILOSOPHY**, am fully aware of the policy of the University relating to the retention and use of higher degree theses, namely that the University retains the copies of any thesis submitted for examination and that the University holds that no thesis submitted for a higher degree should be retained in the library for record purposes only but, within copyright privileges of the author, should be public property and accessible for consultation at the discretion of the Librarian.

In the light of these provisions, I declare that I wish to retain my full privileges of copyright in my thesis and request that neither the whole nor any portion of the thesis may be published by the university Librarian nor may he authorise the publication of the whole or any part of the thesis. I further declare that this preservation of my copyright privileges in the thesis shall lapse from the 30th day of June, 1998 unless it shall previously have been extended or revoked in writing over my hand.

I authorise publication by University Microfilms of a 350 word abstract in Dissertation Abstracts International (DAI).

Signature .....

Witness .....

Date 27 June 1995

TABLE OF CONTENTS

		Page
ABSTRACT		i
ACKNOWLEDGEMENTS		iii
LIST OF FIGURES		iv
LIST OF TABLES		x
CHAPTER ONE:	**INTRODUCTION**	1
	1.1. Location.	1
	1.2. Previous geological investigations.	2
	1.3. Research aims.	3
	1.4. Methods of study.	3
	1.5. Comments on thesis.	3
CHAPTER TWO:	**LATE PRECAMBRIAN STRATIGRAPHY**	5
	2.1. Introduction.	5
	2.2. Morad Formation.	5
	2.2.a. Introduction.	5
	2.2.b. Formation boundaries.	5
	2.2.c. Fossils and age.	6
	2.2.d. Regional aspects and correlation.	6
	2.2.e. Discussion.	8
	2.3. Rizu Formation.	8
	2.3.a. Type section.	8
	2.3.b. Status and relationships.	8
	2.3.c. Formation boundaries.	9
	2.3.d. Fossils and age.	9
	2.3.e. Regional aspects and correlations.	10
	2.3.f. Igneous activity.	11
	2.3.g. Mineralisation.	11
	2.3.h. Tectonic setting.	12
	2.3.i. Discussion.	12
CHAPTER THREE:	**'INFRACAMBRIAN'-CAMBRIAN STRATIGRAPHY**	15
	3.1. Introduction.	15
	3.1.a. Precambrian-Cambrian boundary problems.	15
	3.1.b. Boundary problems in Iran.	15
	3.2. Banestan Formation.	16
	3.2.a. Type section.	16
	3.2.b. Formation boundaries.	17
	3.2.c. Fossils and age.	17
	3.2.d. Regional variation and correlation.	18
	3.3. Soltanieh Formation.	19
	3.3.a. Introduction.	19
	3.3.b. Type section.	19
	3.3.c. Variation in the Alborz Mountains.	20
	3.3.d. Regional aspects.	21
	3.3.e. Discussion.	21
	3.4. Cambrian System.	22
	3.4.a. Introduction.	22
	3.5. Dahu Group.	23
	3.6. Zaigun Formation.	23
	3.6.a. Introduction.	23
	3.6.b. Type section.	23
	3.6.c. Formation boundaries.	23
	3.6.d. Fossils and age.	24

3.6.e. Regional aspects. 24
3.6.f. Depositional environments. 24
3.7. Mohammad Abad Sandstone. 24
3.7.a. Introduction. 24
3.7.b. Type section. 24
3.7.c. Formation boundaries. 26
3.7.d. Fossils and age. 26
3.7.e. Regional aspects. 26
3.8. Lalun Formation. 26
3.8.a. Introduction. 26
3.8.b. Type locality. 26
3.8.c. Formation boundaries. 28
3.8.d. Fossils and age. 28
3.8.e. Regional aspects and correlations. 28
3.9. Khoram Abad Sandstone. 30
3.9.a. Introduction. 30
3.9.b. Type section. 30
3.9.c. Formation boundaries. 30
3.9.d. Regional aspect and correlations. 30
3.9.e. Tectonic setting. 31
3.9.f. Discussion. 31
3.10. Kuhbanan Formation. 31
3.10.a. Previous studies. 31
3.10.b. Type section. 32
3.10.c. Formation boundaries. 32
3.10.d. Fossils and age. 32
3.10.e. Regional aspect and correlations. 32
3.10.f. Discussion. 34
3.11. Hatkan Dolomite. 34
3.11.a. Introduction. 34
3.11.b. Previous studies. 34
3.11.c. Type section. 34
3.11.d. Fossils and age. 35
3.11.e. Formation boundaries. 35
3.11.f. Regional aspects and correlation. 35
3.12. Kalshaneh Formation. 36
3.12.a. Introduction. 36
3.12.b. Formation boundaries. 36
3.12.c. Fossils and age. 36
3.12.d. Regional aspects and correlation. 36
3.12.e. Discussion. 36
3.13. Derenjal Formation. 37
3.13.a. Introduction. 37
3.13.b. Formation boundaries. 37
3.13.c. Fossils and age. 37
3.13.d. Regional aspects and correlations. 38
3.13.e. Discussion. 38

CHAPTER FOUR: ORDOVICIAN STRATIGRAPHY. 39
4.1. Introduction. 39
4.2. Shirgesht Formation. 39
4.2.a. Introduction. 39
4.2.b. Type locality and section. 39
4.2.c. Description. 39
4.2.d. Formation boundaries. 40
4.2.e. Fossils and age. 40
4.2.f. Regional aspects and correlation. 41
4.2.g. Discussion. 42
4.3. Katkoyeh Formation. 43
4.3.a. Introduction. 43
4.3.b. Type section. 43
4.3.c. Lithologies and environments. 43
4.3.d. Formation boundaries. 44
4.3.e. Fossils and age. 44
4.3.f. Regional aspects and correlations. 45

CHAPTER FIVE: SILURIAN STRATIGRAPHY. 47
5.1. Introduction. 47
5.2. Shabdjereh Formation. 47
5.2.a. Type section. 47
5.2.b. Formation boundaries. 48
5.2.c. Fossils and age. 48
5.2.d. Regional aspects and correlation. 49
5.2.e. Discussion. 50
5.3. Niur Formation. 50
5.3.a. Type section. 50
5.3.b. Formation boundaries. 51
5.3.c. Fossils and age. 51
5.3.d. Regional aspects and correlations. 52
5.4. Tectonic setting and regional patterns of sedimentation. 54
5.5. Discussion. 54

CHAPTER SIX: PETROGRAPHY, DIAGENESIS, PROVENANCE STUDIES AND CLUSTER ANALYSIS 55
6.1. Petrography. 55
6.1.a. Introduction. 55
6.1.b. Methodology. 55
6.1.c. Results. 56
6.1.d. Mohammad Abad Sandstone. 58
6.1.e. Lalun Formation. 59
6.1.f. Khoram Abad Sandstone. 59
6.1.g. Katkoyeh Formation. 59
6.1.h. Niur Formation. 60
6.1.i. Shabdjereh Formation. 60
6.2. Diagenesis. 61
6.2.a. Introduction. 61
6.2.b. Methods. 61
6.2.c. Diagenetic processes. 62
6.2.d. Authigenic minerals and cementation. 63
6.2.e. Paragenesis in the Tabas-Kerman region. 65
6.2.f. Discussion. 67
6.3. Provenance studies. 68
6.3.a. Introduction. 68
6.3.b. Precambrian. 69
6.3.c. Cambrian. 69
6.3.d. Ordovician. 70
6.3.e. Silurian. 71
6.3.f. Discussion. 72
6.4. Cluster analysis. 72
6.4.a. Cambrian. 73
6.4.b. Ordovician. 75
6.4.c. Silurian. 76
6.4.d. Discussion. 78

CHAPTER SEVEN: SEDIMENTARY STRUCTURES, PALAEOCURRENT ANALYSIS AND HYDRODYNAMIC INTERPRETATIONS. 81
7.1. Sedimentary structures. 81
7.1.a. Introduction. 81
7.1.b. Depositional structures. 81
7.1.c. Post-depositional structures. 85
7.1.d. Erosional structures. 85
7.1.e. Surface and soil structures. 86
7.1.f. Chemically induced structures. 87
7.1.g. Biogenic sedimentary structures. 88
7.2. Palaeocurrent analysis. 89
7.2.a. Discussion. 90
7.3. Hydrodynamic interpretations. 90
7.3.a. Introduction. 90
7.3.b. Water depth. 91

7.3.c. Width of channel. 92
7.3.d. Dune wavelength. 92
7.3.e. Sinuosity. 92
7.3.f. Flow velocity. 92
7.3.g. Discharge. 93

CHAPTER EIGHT: DEPOSITIONAL ENVIRONMENTS AND FACIES 95
8.1. Introduction. 95
8.2. Previous studies. 95
8.3. Sedimentary facies. 95
8.4. Fluvial systems. 96
8.4.a. Zaigun Formation and Mohammad Abad Sandstone (lower part): alluvial fan assemblage. 97
8.4.b. Mohammad Abad Sandstone (upper part). 99
8.4.c. Discussion. 101
8.5. Marine environments. 101
8.5.a. Coastal and shallow marine environments. 101
8.5.b. Turbidite deposits. 104
8.5.c. Niur and Shabdjereh Formations. 105

CHAPTER NINE: TECTONICS AND SEDIMENTATION 109
9.1. Introduction. 109
9.2. Previous interpretations of the tectonic setting of the study area. 109
9.3. Palaeomagnetic reconstructions. 110
9.4. Tectonics of the study area. 110
9.4.a. Faults. 110
9.4.b. Rifting. 111
9.4.c. Horsts and grabens. 111
9.5. Relationship between tectonics and sedimentation. 112
9.5.a. Evidence used in analysis. 112
9.6. Depositional phases. 113
9.6.a. Introduction. 113
9.6.b. Depositional system I. 113
9.6.c. Depositional system II. 114
9.6.d. Depositional system III. 116
9.6.e. Depositional system IV. 118
9.7. Summary of major tectonic events. 119
9.8. Evidence for eustatic sea level changes. 120
9.8.a. Comparisons with Phanerozoic sea level curves. 120
9.8.b. Sequence stratigraphy. 120
9.9. Regional comparison with Middle East tectonics. 121

CHAPTER TEN: A REVIEW OF THE CAMBRIAN, ORDOVICIAN AND SILURIAN SYSTEMS IN NEIGHBOURING COUNTRIES OF THE MIDDLE EAST 123
10.1. Cambrian. 123
10.1.a. Arabian peninsula. 123
10.1.b. NW Saudi Arabia, southern Jordan and southern Israel. 123
10.1.c. Southern Arabia. 124
10.1.d. Southern Jordan. 124
10.1.e. Oman. 124
10.1.f. Turkey. 125
10.1.g. Afghanistan. 126
10.1.h. Pakistan. 127
10.1.i. Discussion. 127
10.2. Ordovician. 127
10.2.a. Introduction. 127
10.2.b. SE and NW Saudi Arabia. 128

10.2.c. Central Arabia. 128
10.2.d. Southern Jordan. 128
10.2.e. Interior Oman. 129
10.2.f. Turkey. 129
10.2.g. Northern Iraq. 130
10.2.h. Afghanistan. 130
10.3. Silurian. 130
10.3.a. Arabian peninsula. 130
10.3.b. Southern Jordan. 131
10.3.c. Turkey. 131
10.3.d. Afghanistan. 132
10.4. Sedimentation patterns. 132
10.5. Tectonics. 132

CHAPTER ELEVEN: PALAEOGEOGRAPHY AND PALAEOCLIMATES 135
11.1. Palaeogeography. 135
11.1.a. Late Precambrian-Cambrian succession. 135
11.1.b. Cambrian. 136
11.1.c. Ordovician. 136
11.1.d. Silurian. 137
11.1.e. Conclusions. 138
11.2. Palaeoclimates. 138
11.2.a. Introduction. 138
11.2.b. Early Palaeozoic climates in the Middle East. 139
11.2.c. Palaeoclimates of the study area. 141

CHAPTER TWELVE: CONCLUSIONS 143
12.1. Stratigraphy. 143
12.1.a. Late Precambrian-Early Cambrian. 143
12.1.b. Cambrian. 143
12.1.c. Ordovician. 144
12.1.d. Silurian. 144
12.2. Petrography and cluster analysis. 144
12.2.a. Petrography. 144
12.2.b. Cluster analysis. 145
12.3. Provenance. 145
12.3.a. Precambrian. 145
12.3.b. Cambrian. 145
12.3.c. Ordovician. 145
12.3.d. Silurian. 145
12.4. Palaeoclimates. 146
12.4.a. Late Precambrian-Cambrian. 146
12.4.b. Cambrian. 146
12.4.c. Ordovician. 146
12.4.d. Silurian. 146
12.5. Tectonics, depositional environments and facies. 146
12.5.a. Depositional phases. 147
12.5.b. Sea levels. 147
12.5.c. Controls on sedimentation. 147
12.6. Palaeogeography. 149

REFERENCES 151

APPENDICES

Appendix 1. Stratigraphic sections.
Appendix 2. Petrographic data and cluster analysis.
Appendix 3. Standard deviations for provenance.
Appendix 4. Cluster analysis of sandstones.
Appendix 5. Palaeocurrent data.

ABSTRACT

The Kerman-Tabas region of East-Central Iran contains the thickest and most complete sequence of Early Palaeozoic (Cambrian to Silurian) rocks in Iran and the Middle East, but the stratigraphy is complex.

Detailed reassessment of stratigraphic relationships between the Early Palaeozoic strata, together with new sedimentological, petrological and palaeontological data, indicate that the Kerman-Tabas region was tectonically active during this period, not a passive Palaeo-Tethyan shallow marine platform facies as previously suggested. A rift model, involving horst and graben formation, has been invoked to account for the sedimentation patterns in the Late Precambrian to Silurian sequences of the study area. Four phases of extensional (rift) basin development are recognised here, each bounded by a major sequence boundary, with Type I unconformities occurring at the base of: the Rizu Formation; the Dahu Group; the Katkoyeh Formation; and the Shabdjereh and Niur Formations.

Deposition of the Late Precambrian Morad Formation was followed by a period of upwarping and erosion giving an unconformable, but locally faulted, boundary with the overlying Rizu Formation. Bimodal volcanism in the lagoonal to lacustrine Rizu Formation indicates the initiation of rifting. The overlying Ravar and Banestan Formations were deposited in marginal to shallow marine conditions. A scarcity of diagnostic fossils precludes precise location of the Precambrian-Cambrian boundary in the study area but supratidal to intertidal conditions in the Upper Dolomite Member of the Soltanieh Formation and in the Barut Formation indicate a low stand sea-level in the Early Cambrian. Cambrian strata in the Kerman region, assigned to the Dahu Group (redefined), include the Zaigun Formation, Mohammad Abad Sandstone (new name), Lalun Formation (redefined) and Khoram Abad Sandstone (new name). Lake facies in the Zaigun Formation and fluvial sequences in the Mohammad Abad Sandstone followed extensional tectonic activity and inter-continental basin deposition. Different palaeocurrent trends E and W of the Kuhbanan Fault indicate that this fault was active during deposition. A transgression in the late Early Cambrian formed a ravinement surface at the base of the Lalun Formation overlain by aeolian and beach sandstone. This was followed by supratidal and intertidal facies in the Lalun Formation and a barrier island system in the Khoram Abad Sandstone, indicating progradation and a relatively high sediment input. The Kuhbanan Formation (maximum flooding surface) represents a deeper water facies in the Kerman area in southern Iran than the time-equivalent lagoonal facies in the Kalshaneh Formation near Tabas and the supratidal-intertidal facies in Member 1 of the Mila Formation in the Alborz Mountains. Late Cambrian regressive, shallowing-upwards carbonate facies accumulated in the Kerman region, while relatively deeper water facies characterised the Derenjal Formation in the Tabas area and the Mila Formation in the Alborz Mountains.

New palaeontological data indicate that the previously poorly defined Cambrian-Ordovician boundary is located in the uppermost carbonate facies of the Derenjal Formation at Dahaneh-e-Kolut, Tabas area. Intense Early Ordovician subsidence in the Tabas region led to deposition of the thick siliciclastic and carbonate facies of the Tremadoc Shirgesht Formation, compared with the thin carbonate facies of Member 5 of the Mila Formation in the Alborz Mountains. The Katkoyeh Formation is proposed to accommodate the Ordovician of the Kerman area, where it contains Arenig to Ashgill faunas including the graptolite *Dictyonema ghodsiae* Rickards *et al.* 1994; Arenig trilobites are reported for the first time from the Kalmard region from this formation. Pillow basalt of continental origin in the basal Katkoyeh Formation indicates a period of extensional rifting. The Early Arenig transgression of this formation in the Kalmard and Kerman regions, and probably into the Alborz Mountains (Lashkerak Formation), may indicate contemporaneous rift development and a high stand sea-level. Transgressive-regressive sequences in the upper Katkoyeh Formation near Kerman indicate sea-level fluctuations.

This Early Palaeozoic extensional phase led to deposition of the relatively thick Shabdjereh Formation near Kerman, and terminated in the Early Silurian. The laterally equivalent Niur Formation at Dahaneh-e-Kolut is faulted against the Shirgesht Formation; elsewhere it has a disconformable contact with the underlying Cambrian Derenjal Formation. Extrusion of pillow basalt in the lower Niur Formation can be traced into the NE Alborz Mountains. A basal red bed sequence containing hyaloclastite facies is described for the first time, and a barrier island system occurs in the lower part of the Niur Formation. Two non-marine horizons and several polymictic conglomerate lenses highlight absence of deep marine facies in the Shabdjereh Formation in the Kerman region.

Eustatic sea level changes recorded in the studied sequences are: high stands in the late Early Cambrian and the Early Silurian; a global transgression in the Tremadoc; a further rise in the Arenig; and a regression at the end of the Ordovician.

Provenance studies indicate a major cratonic source for the study area in the Early Palaeozoic with periodic detritus from nearby volcanic sources. Throughout the Early Palaeozoic palaeo-relief in the Kerman area was greater than that in the Tabas area.

A warm, low latitude climate during the Early Palaeozoic of Iran is indicated by red beds, evaporites, mudcracks, salt and gypsum pseudomorphs, caliche and stromatolites seen to varying degrees throughout the Cambrian-Silurian succession. This contrasts with the glacial deposits in the Late Ordovician-Silurian strata of the Arabian Peninsula.

The study area and the Arabian Peninsula have a similar Late Precambrian and Cambrian tectonic style. Different Ordovician and Silurian faunas, palaeoclimates and tectonic conditions distinguish East-Central Iran from Saudi Arabia, but there was a close relationship between Iran, Afghanistan and Turkey.

ACKNOWLEDGEMENTS

This thesis would not have been successfully completed without the support of my family, and that of the academic and support staff of the Department of Geology.

This study was undertaken with the assistance of a scholarship from the Ministry of Mines and Metals, and the Ministry of Culture and Higher Education of the Islamic Republic of Iran.

For their guidance throughout the study, I would like to express my deep appreciation to my supervisors Associate Professor Brian Jones, Head of the Discipline of Geology, and Associate Professor Tony Wright, former Head of the Department of Geology who assisted with transportation of rock samples. Dr Paul Carr kindly provided analyses and age determinations for igneous rocks. I am grateful to all other academic, administrative and technical staff of the department for their assistance.

The author also wishes to thank: Dr Iradj Yassini for his encouragement. Special thanks are also extended to Dr Hamdi, Dr Golshani, Professor Art Boucot, Professor David Bruton, Professor Brian Chatterton, Dr Peter Jones, Dr Bob Nicoll, Dr Barrie Rickards and Professor June Ross for accurate age determinations of Iranian fossils; Dr Clinton Foster for processing samples for acritarchs and supplying photographs of specimens that were recovered; Professor John Talent who made MUCEP facilities available; Dr Susanne Pohler for help with translation; and Dr Theresa Winchester-Seeto for her generous assistance with preparation of Iranian palynomorphs.

Many thanks are also addressed to all my post-graduate colleagues, especially Kerri Bann for lively discussion.

LIST OF FIGURES

Chapter 1.

Figure 1.1. Principal geological elements of Iran.
Figure 1.2. General topographic map of Iran showing major deserts and traces of major faults (black points).
Figure 1.3. Location of the study areas and the main accessibility.
Figure 1.4. Correlation of Precambrian to Early Palaeozoic sequences of northern Iran and East-Central Iran (after Stöcklin & Setudehnia 1972).
Figure 1.5. Towns, cities and other localities mentioned in the text.

Chapter 2.

Figure 2.1. Disconformable contact between the Morad and Rizu Formations in the Ab-e-Morad area.
Figure 2.2. Contact metamorphic spots in Morad Formation, incident light, x2.5.
Figure 2.3. Core of spot, showing tourmaline, crossed polars, x10.
Figure 2.4. Angular unconformity between terrigenous, probably non-marine, facies of the upper Kalmard and Kuhbanan Formations, Rahdar section.
Figure 2.5. Tourmaline-bearing contact metamorphosed Katkoyeh Formation, Rahdar section. Crossed polars, x6.3.
Figure 2.6. Spiny fragments of broken and spherical, granular-walled acritarchs. Bar scale = 100 μ. Photographs by Dr C. Foster, AGSO.

Chapter 3.

Figure 3.1. World-wide commercial Precambrian-Cambrian phosphorite belt (dashed, after Brasier *et al.* 1989).
Figure 3.2. Correlation chart for the Late Precambrian to Early Cambrian of various regions including SW Asia (after Brasier 1989).
Figure 3.3. General view of the Banestan Formation in contact with the Rizu formation E of Zarand.
Figure 3.4. General view of the upper part of the Mohammad Abad Sandstone, type locality, Kerman area.
Figure 3.5. General view of the Lalun Formation (Lower Sandstone Unit left, Khoram Abad Sandstone right), 750 m S of Mohammad Abad village.
Figure 3.6. Erosional contact between Khoram Abad Sandstone (left) and overlying dolomitic Banestan Formation (right), both overturned; Kuhbanan area.
Figure 3.7. Gypsiferous facies of Kuhbanan Formation, Shabdjereh area.
Figure 3.8. General view of Kuhbanan Formation (right), Hatkan Dolomite (middle) and Shabdjereh Formation (left), Shabdjereh area.
Figure 3.9. Sections through the Banestan Formation; a, Veraoun valley; b, 25 km NW of Zarand; c, S of Behabad.
Figure 3.10. Columnar section through the Soltanieh Formation, Tabas area.
Figure 3.11. Columnar section through the Zaigun Formation, Kerman area.
Figure 3.12. Geological map of the Shabdjereh area, showing type sections of all the formations of the Dahu Group and the Shabdjereh Formation.
Figure 3.13. Columnar section of the Lalun Formation, Shabdjereh area.
Figure 3.14. Vertical and planar views of stromatolites from the Lalun Formation, Tabas area.
Figure 3.15. Columnar section of the Lalun Formation, Tabas area.
Figure 3.16. Columnar sections of the Kuhbanan Formation, Kerman area; a, W of Shabdjereh; b, Givi area (both W of Kuhbanan Fault); c, Kuhbanan (E of Kuhbanan Fault).

Chapter 4.

Figure 4.1. Columnar sections through the Shirgesht Formation: a, at Chah-e-Baba Ali; b, at Dahaneh-e-Kolut.
Figure 4.2. Trilobites from the Shirgesht Formation, Dahaneh-e-Kolut.
Figure 4.3. Transgressive and regressive facies in the Katkoyeh Formation, Khoda Afarin area, Kerman.
Figure 4.4. Pillow basalt in the lower part of the Katkoyeh Formation, Katkoyeh area, Kerman.

Figure 4.5. Regressive flood plain facies, Katkoyeh Formation, Khoda Afarin area, Kerman.
Figure 4.6. Stromatolitic clast in the basal Katkoyeh Formation, Shabdjereh area.
Figure 4.7. Measured sections through the lower part of the Katkoyeh Formation, Shabdjereh area. a, b, W of the Kuhbanan Fault; c, E of the Kuhbanan Fault; d, Khoda Afarin area.
Figure 4.8. The graptolite *Dictyonema ghodsiae* Rickards, Hamedi & Wright, 1984, from the lower part of the Katkoyeh Formation.
Figure 4.9. Measured sections through the Katkoyeh Formation, Kalmard area. a, Darin area; b, Chah-e-Mohammad area; c, Rahdar area.
Figure 4.10. *Cruziana* from the Katkoyeh Formation, Tabas area.

Chapter 5.

Figure 5.1. Columnar sections of the Shabdjereh Formation, Shabdjereh area, Kerman region. a, 10 km W of Shabdjereh; b, the type locality.
Figure 5.2. General view of disconformity between the basal fluvial system of the Shabdjereh Formation (A, B, left) and Hatkan Dolomite (H, right), at the Shabdjereh type section. A, channel deposits, B floodplain deposits.
Figure 5.3. Caliche facies in basal Shabdjereh Formation, floodplain facies.
Figure 5.4. General view of the upper red sequences (non-marine) at type locality of the Shabdjereh Formation.
Figure 5.5. Unbranched stromatolite in the Shabdjereh Formation, E of the Kuhbanan Fault, in the Khoda Afarin section.
Figure 5.6. Columnar section of the Shabdjereh Formation, 10 km N of Shabdjereh.
Figure 5.7. Columnar section of the Shabdjereh Formation in the Khoda Afarin area, E of the Kuhbanan Fault.
Figure 5.8. Columnar sections of the Niur Formation in the Dahaneh-e-Kolut area, Tabas region. a, W side of Dahaneh-e-Kolut; b, c, lower part, on E side of Dahaneh-e-Kolut.
Figure 5.9. Ostracod in the basal sandstone of the Niur Formation, W side (section 5.8a) of Dahaneh-e-Kolut, Tabas region.
Figure 5.10. General view of the red beds and gypsiferous facies in the lower part (section 5.8c) of the Niur Formation, E side of Dahaneh-e-Kolut.
Figure 5.11. Disconformable contact between the Derenjal Formation (left) and hyaloclastite facies of Niur Formation (right), E side of Dahaneh-e-Kolut.
Figure 5.12. Isolated (lava) pillow in the lower part of the Niur Formation, E side of the Dahaneh-e-Kolut area, Tabas region.
Figure 5.13. Rich assemblage of trilobites and brachiopods in the Niur Formation, Dahaneh-e-Kolut, Tabas region.
Figure 5.14. Trilobites from the Niur Formation (Silurian), Dahaneh-e-Kolut.

Chapter 6.

Figure 6.1. Triangular diagrams for sandstone classification (Folk 1980).
Figure 6.2. Contact-metamorphic tremolite-bearing clast, Lalun Formation, Tabas area.
Figure 6.3. Biotite, apatite and microcline in a clast in the Lalun Formation, Shabdjereh.
Figure 6.4. Clast containing quartz vacuoles, Shirgesht Formation, Dahaneh-e-Kolut.
Figure 6.5. Boehm lamellae in quartz grain in the Katkoyeh Formation, Tabas area, Rahdar section.
Figure 6.6. Metamorphic quartz clast, basal fluvial system, Shabdjereh Formation, Kerman area.
Figure 6.7. Chert clasts, iron coating, quartz overgrowth and sericite cement, Mohammad Abad Sandstone (zircon grain lower left), Kerman area.
Figure 6.8. Volcanic clasts, altered feldspar, carbonate and chlorite cement, upper red sequences, Shabdjereh Formation, Kerman region.
Figure 6.9. Quartz-zircon clast from an igneous source, with an altered feldspar clast, fluvial facies, Shabdjereh Formation, Kerman region.

Figure 6.10. Tourmaline and microcline overgrowths, Lower Sandstone, Niur Formation, Tabas region.
Figure 6.11. Authigenic carbonate cement in the form of caliche, floodplain sandstone, Shabdjereh Formation, Shabdjereh.
Figure 6.12. Feldspar overgrowth and iron oxide cement, basal fluvial system, Shabdjereh Formation, Shabdjereh.
Figure 6.13. Replacement of labile materials by carbonate, chlorite and quartz, Shabdjereh Formation, Kerman area.
Figure 6.14. Diagenetic relationship between depth and temperatures (after Douglas *et al.* 1994).
Figure 6.15. An example of whole-rock XRD analysis for the Mohammad Abad Sandstone (AH-10.4).
Figure 6.16. Standard triangular diagrams showing distribution of mean detrital modes for sandstone suites derived from different types of provenances (after Dickinson 1985).
Figure 6.17. Triangular diagrams showing provisional compositional fields of sand derived from different types of provenance (after Dickinson 1985).
Figure 6.18. QFL and QmFLt triangular diagrams showing compositional variation of sandstones from the Mohammad Abad Sandstone (a, b) in the Kerman area, and the Lalun Formation and Khoram Abad Sandstone (c, d: both Tabas area).
Figure 6.19. QFL and QmFLt triangular diagrams showing compositional variation of sandstones from the Katkoyeh Formation; a, b, from the Shabdjereh area, and c, d, from the Katkoyeh area.
Figure 6.20. QFL and QmFLt triangular diagrams showing compositional variation of sandstones from the Katkoyeh Formation; a, b, from the Darin area, and c, d, from the Rahdar area.
Figure 6.21. QFL and QmFLt triangular diagrams showing compositional variation of sandstones from the Shabdjereh Formation; a, b, from the Shabdjereh area, and c, d, from the Khoda Afarin area.
Figure 6.22. QFL and QmFLt triangular diagrams showing compositional variation of sandstones from the Niur Formation, from the Tabas area.
Figure 6.23. Q-mode (a) and R-mode (b) dendrograms for Cambrian sandstones.
Figure 6.24. R-mode dendrogram for sandstones of the Mohammad Abad Sandstone, Tabas region.
Figure 6.25. Q-mode (a) and R-mode (b) dendrograms for sandstones of the Lalun Formation, Tabas area.
Figure 6.26. Q-mode dendrogram for Ordovician sandstones.
Figure 6.27. R-mode dendrogram for Ordovician sandstones.
Figure 6.28. Q-mode (a) and R-mode (b) dendrograms for sandstones of the Katkoyeh Formation, Tabas region.
Figure 6.29. Q-mode dendrogram for Silurian sandstones.
Figure 6.30. a) R-mode dendrogram for Silurian sandstones; (b) Q-mode and c, R-mode dendrograms for Niur Formation sandstones, Tabas area.

Chapter 7.

Figure 7.1. Two sets of symmetrical ripples with rounded crests in the Katkoyeh Formation, Tabas region.
Figure 7.2. Bifurcation wave ripples in lake deposits of the Mohammad Abad Sandstone, type locality.
Figure 7.3. Interference ripples associated with mudcracks in the Shabdjereh Formation, Kerman.
Figure 7.4. Double-crested ripple marks associated with reduction spot in the Lalun Formation, Kerman region.
Figure 7.5. Flaser and lenticular bedding in the Lalun Formation, Kerman region. R indicates ripple cross-lamination.
Figure 7.6. Herringbone and planar cross-bedding in the upper part of the Derenjal Formation, Tabas area.
Figure 7.7. Small linguoid ripples in the Katkoyeh Formation (current lower left to upper right), Tabas area.

Figure 7.8. Megaripples in the Hatkan Dolomite (Dorah-e-Shah Dad section), Kerman area.
Figure 7.9. Recumbent, trough and planar cross-bedding in the Katkoyeh Formation, Tabas area.
Figure 7.10. Undulating bedding in the Mohammad Abad Sandstone, Kerman area.
Figure 7.11. Swaley and hummocky cross-stratification in the Katkoyeh Formation, Tabas area.
Figure 7.12. Bouma sequences in the Shirgesht Formation, Tabas area.
Figure 7.13. Monroe structures in the tidal flat facies, Lalun Formation, Kerman area.
Figure 7.14. Load casts in the Lalun Formation, Kerman area.
Figure 7.15. Ball and pillow structures in the Katkoyeh Formation, Tabas area.
Figure 7.16. Flute casts and bioturbation in the Katkoyeh Formation, Tabas area.
Figure 7.17. Scour-and-fill structures in amalgamated sequences, Mohammad Abad Sandstone, Kerman area.
Figure 7.18. Gutter casts in the Mohammad Abad Sandstone, Kerman area.
Figure 7.19. Down-cutting structure in the fluvial system of the Mohammad Abad Sandstone, Kerman area.
Figure 7.20. Desiccation mudcracks in the Lalun Formation, Kerman area.
Figure 7.21. Synaeresis mudcracks, Shabdjereh Formation, Kerman area.
Figure 7.22. *Arenicolites* associated with interference ripples in the Katkoyeh Formation, Tabas area.
Figure 7.23. *Palaeophycus*, Niur Formation, Tabas area.
Figure 7.24. *Skolithos*, Katkoyeh Formation, Tabas area.
Figure 7.25. Distribution of typical ichnofacies (Frey 1990).
Figure 7.26. a, *Diplocraterion* in the upper part of the Derenjal Formation; b, *Didymaulichnus* (a), and *Bergaueria* (b) from non-marine beds, Shabdjereh Formation, Kerman area.
Figure 7.27. Palaeocurrents for the Banestan Formation (a) S of Ravar, (b) N of Zarand; the Lalun Formation (c) aeolian beds, (d) tidal flat facies, Kerman area, and (e) tidal flat facies, Tabas area; (f) Khoram Abad Sandstone, Kerman area.
Figure 7.28. Columnar section of the Mohammad Abad Sandstone showing palaeocurrents and major facies, from type locality, Kerman.
Figure 7.29. Palaeocurrents for the Katkoyeh Formation; (a) Rahdar section; (b) Darin section; (c) Chah-e-Mohammad section.
Figure 7.30. Palaeocurrents for: the Shabdjereh Formation; (a) type locality, Shabdjereh; and (b) 10 km N of Shabdjereh; and (c) Niur Formation, Tabas area.
Figure 7.31. Columnar section of the basal non-marine part of the Shabdjereh Formation, showing palaeocurrents and major facies, from type locality, Kerman.
Figure 7.32. Pattern of palaeocurrents in Mohammad Abad Sandstone; A, type locality W of Kuhbanan Fault and B, E of the Kuhbanan Fault, Kerman area.
Figure 7.33. Size-velocity diagram generated by flume experiments, using a flow depth of 0.4 m (after Southard *et al.* 1990).

Chapter 8.

Figure 8.1. Relationship between facies, depositional environments and depositional systems (after Walker 1992).
Figure 8.2. Reconstruction of the Zaigun Formation and the lower part (alluvial fan sequence) of the Mohammad Abad Sandstone.
Figure 8.3. Gm and Gh facies in the alluvial fan of the Mohammad Abad Sandstone, type locality, Kerman region.
Figure 8.4. St and Sm facies in the Mohammad Abad Sandstone, Kerman area.
Figure 8.5. Lag deposits (Glg facies, as well as Gm, Sm, Gh facies) in the basal alluvial fan of the Shabdjereh Formation, Kerman area.
Figure 8.6. Low angle planar cross-bedding and Sh, St, Sl and Fl facies in the bar of Mohammad Abad Sandstone.

Figure 8.7. Flood plain facies in the Mohammad Abad Sandstone, Kerman area.
Figure 8.8. General view of the playa lake facies of the Mohammad Abad Sandstone (faces to the N), Kerman area.
Figure 8.9. Primary lineations in the Mohammad Abad Sandstone, Kerman area.
Figure 8.10. Cyclic, fining- and thinning-upwards sequences in the sandy river deposits, Mohammad Abad Sandstone, Kerman area.
Figure 8.11. Monomictic conglomerate in the channel bar of the basal fluvial system of the Shabdjereh Formation, at the type locality, Kerman region.
Figure 8.12. Planar and trough cross-bedded sandstone (Sp and St facies) of the sandy river, Mohammad Abad Sandstone, Kerman area.
Figure 8.13. Reactivation surfaces in the bar of Mohammad Abad Sandstone, Kerman region.
Figure 8.14. Angular unconformity in reoccupied channel in the Mohammad Abad Sandstone, Kerman region.
Figure 8.15. Columnar section through playa lake sequence of the Mohammad Abad Sandstone, showing cyclicity and heterolithic facies, Kerman area.
Figure 8.16. Different lithofacies in the representative fining-upwards sandy river sequence of the Mohammad Abad Sandstone, Kerman area.
Figure 8.17. Depositional environments and facies associations of marine upper part of the Dahu Group (Lalun Formation and Khoram Abad Sandstone) and Kuhbanan Formation.
Figure 8.18. Planar beach and aeolian facies in the Lower Sandstone Unit, Lalun Formation, new type locality, Kerman.
Figure 8.19. Ravinement facies in the Lower Sandstone Member, Lalun Formation, new type locality, Kerman.
Figure 8.20. Large-scale cross lamination in the Khoram Abad Sandstone, Kerman area.
Figure 8.21. Sigmoidal tidal bundles in the lower part of the Katkoyeh Formation, Tabas area.
Figure 8.22. Carbonates representing high and low energy environments in the upper part of the Derenjal Formation, Tabas area.
Figure 8.23. Low angle cross-bedding in the Lower Sandstone Unit of the Niur Formation, Dahaneh-e-Kolut, Tabas area.
Figure 8.24. Classification of channel patterns (a) after Miall (1977) and (b) after Brice (1984).
Figure 8.25. Basal portion of the Shabdjereh Formation, Shabdjereh; fluvial system different lithofacies and several caliche horizons.

Chapter 9.

Figure 9.1. Palaeomagnetic reconstruction of Gondwanaland (Wensink 1983), showing polar wander curve, and Iran between Afghanistan and Oman.
Figure 9.2. Position of continents and glacial domains during Late Ordovician (after Vaslet 1991).
Figure 9.3. Lut Block and Farah Block with flanking basins prior to anticlockwise rotation in Late Palaeozoic-Early Mesozoic, showing Late Precambrian volcanics of the Rizu Formation, and major faults; after Davoudzadeh *et al.* (1981) and Wensink (1991).
Figure 9.4. Ordovician tectonic setting and major structural elements of eastern Iran; Tabas Block bounded by the Nayband, Great Kavir and Nain-Deshir-Hajiabad Faults; other major faults, Precambrian blocks (horizontal lines), and horsts and grabens shown.
Figure 9.5. Model for tectonic and sedimentological evolution of Late Precambrian and Early Cambrian of the study area (modified after Ellis & McClay 1988, and Mitchell & Reading 1986, fig. 14.9).
Figure 9.6. Pre-Quaternary sea level curves (after Hallam 1984); A, Hallam and B, Vail.
Figure 9.7. Rare earth analytical results for basalt from Katkoyeh Formation; multi-element diagram normalised to primordial mantle (after Woods *et al.* 1979).
Figure 9.8. Distribution of Ordovician volcanics and non-volcanic sequences in Iran.

Figure 9.9. Distribution of Silurian volcanics and non-volcanic sequences in Iran.
Figure 9.10. Ordovician sea level curve, after Ross & Ross (1992).
Figure 9.11. Worldwide sea-level changes during the Silurian (after Johnson & McKerrow 1991).
Figure 9.12. N-S trend of the major fold structures and oil fields in the Saudi-Arabia Platform (Edgell 1987, 1990).

Chapter 10.

Figure 10.1. Major tectonic elements in Afghanistan (after Wensink 1991).

Chapter 11

Figure 11.1. The palaeogeography and biogeography of the Cambrian (after Boucot & Gray 1986).
Figure 11.2. (a), Ordovician realms; and (b), oceanic circulation patterns; based on coral, stromatoporoid and reef distributions (after Webby 1992).
Figure 11.3. Ordovician palaeogeography and biogeography (after Boucot & Gray 1986).
Figure 11.4. Lower Silurian palaeogeography and biogeography (after Boucot & Gray 1986).
Figure 11.5. Upper Silurian palaeogeography and biogeography (after Boucot & Gray 1986).
Figure 11.6. Silurian palaeoclimates, based on *Catenipora* (Hubman 1991); the number 10 denotes Iran.

Chapter 12.

Figure 12.1. Three major basin categories (after Selley 1985).
Figure 12.2. Tectonic basin classification (after Mitchell & Reading 1986).
Figure 12.3. Distribution of the different facies of the uppermost Precambrian and Cambrian in Iran.
Figure 12.4. Widespread 'old' Lalun (Zaigun Formation, Mohammad Abad Sandstone and Lalun Formation) in Iran.

LIST OF TABLES

Table 1.1.	Abbreviations used in text and diagrams.
Table 1.2.	Symbols used in columnar sections.
Table 2.1.	Correlation chart for the Morad Formation.
Table 2.2.	Correlation chart for the Rizu Formation.
Table 3.1.	Correlation chart for the Banestan Formation.
Table 3.2.	Correlation chart for the Zaigun Formation.
Table 3.3.	Correlation chart for the Lalun Formation.
Table 3.4.	Correlation chart for the Kuhbanan Formation.
Table 3.5.	Correlation chart for the Hatkan Dolomite.
Table 3.6.	Correlation chart for the Derenjal Formation.
Table 4.1.	Correlation chart for the Shirgesht Formation.
Table 4.2.	Correlation chart for the Katkoyeh Formation.
Table 5.1.	Correlation chart for the Shabdjereh Formation.
Table 6.1.	Summary of XRD analyses for Late Precambrian and Cambrian strata from the study area.
Table 6.2.	Summary of XRD analyses for Ordovician strata from the study area.
Table 6.3.	Summary of XRD analyses for Silurian strata of the study area.
Table 6.4.	R-mode comparison of averaged petrographic data from the Mohammad Abad Sandstone in the Kerman area (a) and the Lalun Formation in the Tabas area (b).
Table 6.5.	R-mode comparison of petrographic data for the Niur Formation beach facies (Tabas area) with Shabdjereh Formation fluviatile facies (Kerman area).
Table 6.6.	Summary of provenance data for Late Precambrian and Early Cambrian formations in the study area.
Table 8.1.	Lithofacies codes used in this study.
Table 9.1.	Geochemical data from pillow basalt (AH - 9-58) from the Katkoyeh Formation, E side of the Kuhbanan Fault, Kerman area.
Table 9.2.	Age data for the Naini Granodiorite in the Kalmard area (493 Ma).
Table 10.1.	Correlation chart for the Cambrian System in the Middle East.
Table 10.2.	Correlation chart for the Ordovician System in the Middle East.
Table 10.3.	Correlation chart for the Silurian System in the Middle East.
Table 12.1.	Correlation and major depositional environments of Late Precambrian and Early Palaeozoic sequences in Iran.